

# Series solution of stagnation slip flow and heat transfer by means of the homotopy analysis method

CHENG Jun<sup>1</sup>, LIAO ShiJun<sup>2</sup>, R. N. MOHAPATRA<sup>3</sup> & K. VAJRAVELU<sup>3</sup><sup>1</sup> Shanghai Institute of Applied Mathematics and Mechanics, Shanghai University, Shanghai 200072, China;<sup>2</sup> State Key Lab of Ocean Engineering School of Naval Architecture, Ocean and Civil Engineering Shanghai Jiao Tong University, Shanghai 200030, China;<sup>3</sup> Department of Mathematics, University of Central Florida, Orlando, FL32816, USA

**An analytical approximation for the similarity solutions of the two- and three- dimensional stagnation slip flow and heat transfer is obtained by using the homotopy analysis method. This method is a series expansion method, but it is different from the perturbation technique, because it is independent of small physical parameters at all. Instead, it is based on a continuous mapping in topology so that it is applicable for not only weakly but also strongly nonlinear flow phenomena. Convergent  $[m,m]$  homotopy Padé approximants are obtained and compared with the numerical results and the asymptotic approximations. It is found that the homotopy Padé approximants agree well with the numerical results. The effects of the slip length  $\ell$  and the thermal slip constant  $\beta$  on the heat transfer characteristics are investigated and discussed.**

stagnation slip flow, Navier boundary condition, nano-fluidics, heat transfer, homotopy analysis method

Stagnation flow on a surface is of great importance in many convection cooling processes<sup>[1]</sup>. In Prandtl boundary layer theory<sup>[2]</sup>, the fluid is assumed to be at rest relative to the solid wall. For macroscopic applications such a no-slip condition is undoubted but recently a number of experiments suggested a violation of the no-slip boundary condition at micro and nano scales<sup>[3-6]</sup>. Instead of the no-slip boundary condition, Navier<sup>[7]</sup> first introduced a slip boundary condition where the slip velocity near the wall is proportional to the local shear stress, i.e.,

$$u = \ell \frac{\partial u}{\partial n}, \quad (1)$$

where  $u$  is the tangential velocity,  $n$  is the normal vector to the plate, and  $\ell > 0$  is the constant slip length, which equals in the magnitude of the fictitious distance below the surface where the no-slip boundary condition would be satisfied. As a matter of fact, the Navier boundary condition and the no-slip boundary condition proposed by Bernoulli and Stokes came into being almost in the

same period. However, it was not until the late 20th century that the Navier boundary condition was re-recognized by the academic circles and industry thanks its application in the nano science and technology.

Theoretical and experimental studies show that the slip on the solid interface has two forms of appearance. One is the so-called molecular or intrinsic slip. For the gaseous nano fluid, when the Knudsen number, the ratio of the molecular mean free path length to a representative physical length scale, is between  $10^{-3} < Kn < 10^{-1}$ , according to the classification of Schaaf and Chambre<sup>[8]</sup>, the gas-fluid enters the slip-flow and thermal jump regime. Also, the experiences<sup>[3,9]</sup> show that if the shear force on the fluid-solid interface reaches a certain threshold, like the plastic flow in the solid mechanics, the liquid molecules will slip along the solid

Received June 30, 2008; accepted March 1, 2009

doi: 10.1007/s11433-009-0117-y

†Corresponding author (email: sjliao@sjtu.edu.cn)

Supported by the National Natural Science Foundation of China (Grant No. 10872129)

interface. Since the fluid velocity on the solid interface does not equal zero, the molecular slip is the real slip. The second form of appearance is the so-called apparent slip. Different from the molecular slip, from the micro-scale point of view, the flow does not slip along the solid interface. Instead, it forms a singular layer on the solid interface where the fluid velocity profile increases with a large gradient from zero on the solid to where the no-slip condition appears to be invalid. Because of its very thin thickness, it is reasonable to regard the maximum velocity to be the slip velocity. Thus, it is called the apparent slip. Examples belonging to this category are electrokinetics<sup>[10]</sup> and acoustic streaming<sup>[11]</sup>, etc. In general, no matter which kind of the slip appearance is, from the theoretical and engineering point of view, the micro and nano boundary-layer flow problem can be presented by the Navier-Stokes equation subject to the Navier slip boundary condition.

In this paper we obtain similar solutions for the stagnation slip flows under the Navier boundary condition. Two-dimensional and three-dimensional flows are considered. For the two-dimensional stagnation flow, the Cartesian coordinate system is used, where  $x$  is measured along the plate and  $y$  normal to it. The velocities  $u$ ,  $v$  are along the  $x$  and  $y$ -axis respectively. The velocity distribution for the potential flow in the neighborhood of the stagnation point at  $x=y=0$  is given by

$$U = ax, \quad V = -ay, \quad (2)$$

where  $a$  is a constant. By the similarity transform:

$$u = ax f'(\eta), \quad v = -\sqrt{va} f(\eta), \quad \eta = \sqrt{\frac{a}{\nu}} y, \quad (3)$$

the Navier-Stokes equation leads to

$$f''' + ff'' - (f')^2 + 1 = 0, \quad (4)$$

where  $\nu$  is the kinematic viscosity and the prime denotes differentiation with respect to  $\eta$ . For the three-dimensional axisymmetric flow, we shall use the cylindrical coordinates  $(r, \phi, y)$  and assume the solid wall is located at  $y=0$ , the stagnation point is located at the origin and that the flow is in the direction of the negative  $y$ -axis. The potential velocity field is

$$U = ar, \quad V = -2ay. \quad (5)$$

Let  $u$ ,  $w$  be the radial and the axial velocity components respectively. The similarity transform:

$$u = arf'(\eta), \quad w = -2\sqrt{va} f(\eta), \quad (6)$$

reduces the Navier-Stokes equation to

$$f''' + 2ff'' - (f')^2 + 1 = 0. \quad (7)$$

The boundary conditions for the two-dimensional and the three-dimensional flows reduce to

$$f'(\infty) = 1, \quad f(0) = 0, \quad f'(0) = \ell^* f''(0), \quad (8)$$

where  $\ell^* = \ell \sqrt{a/\nu}$ . Asterisk denotes the dimensionless variable and will be dropped from here afterwards.

Let the temperature far from the plate be  $T_\infty$  and the temperature on the plate be  $T_0$ . Introduce a dimensionless temperature  $\theta(\eta)$  as

$$\theta = \frac{T - T_\infty}{T_0 - T_\infty}. \quad (9)$$

The energy equation in the nondimensional form becomes

$$\theta'' + Pr f \theta' = 0, \quad (10)$$

for the two-dimensional flow and

$$\theta'' + 2 Pr f \theta' = 0, \quad (11)$$

for the three-dimensional axisymmetric flow, where  $Pr$  is the Prandtl number, which is interpreted as the relative thickness of the velocity and the thermal boundary layers:  $Pr = 1$  gives boundary layers of equal thickness,  $Pr > 1$  gives a thinner velocity boundary layer as momentum transfer is more rapid than heat transfer. For the temperature, the jump boundary condition developed by von Smoluchowski<sup>[12]</sup> is generally applied at the micro and nano scale, and may be written as

$$T - T_0 = \beta T_y, \quad (12)$$

where  $\beta$  is a proportionality constant<sup>[6,13,14]</sup>. The substitution of eq. (9) into (12) yields

$$\theta(0) = 1 + \beta^* \theta'(0), \quad (13)$$

where  $\beta^* = \beta \sqrt{a/\nu} / (T_0 - T_\infty)$  is the thermal slip constant. The asterisk will be dropped from here afterwards. The appropriate boundary condition at infinity is

$$\theta(\infty) = 0. \quad (14)$$

The existence of a similar solution for the stagnation flows with slips has been studied by Ishimura and Ushijima<sup>[15]</sup>. However, generally speaking, we encounter considerable mathematical difficulties in obtaining the exact solution for the boundary layer flow; so that it can only be obtained by numerical method or series expansion methods. Among the commonly-used series expansion methods, the perturbation method<sup>[16-23]</sup> is one of the most successful ones. Nowadays, it has been

widely applied to many aspects of nonlinear science and engineering. The perturbation theory features in its clear physical description, so that it helps people better to understand the nonlinear problems. Through the perturbation analysis, Wang<sup>[13]</sup> obtained the asymptotic property for large  $\ell$ :

$$\theta'(0) \sim -\frac{\sqrt{2 Pr/\pi}}{1 + \beta\sqrt{2 Pr/\pi}}, \quad (15)$$

for two-dimensional flow and

$$\theta'(0) \sim -\frac{2\sqrt{Pr/\pi}}{1 + 2\beta\sqrt{Pr/\pi}}, \quad (16)$$

for axisymmetric flow. However, as all scientific methods, the perturbation method has its limitations as well. It is dependent upon the expansion of a small/large parameter so that it may fail when there is no small/large parameter or the parameter is not sufficiently small/large, as pointed out by Poincaré<sup>[24]</sup>. To overcome this problem, various non-perturbation methods came into being, such as the Lyapunov artificial small parameter method<sup>[25]</sup>, the  $\delta$ -expansion method<sup>[26,27]</sup> and the Adomian decomposition method<sup>[28-31]</sup>. In 1992, Liao proposed a new analytic method for nonlinear problems, namely the homotopy analysis method<sup>[32]</sup>. It is independent of any small/large physical parameters at all. Besides, it is also a unified method logically containing the above-mentioned non-perturbation methods. Furthermore, it can be elegantly combined with many mathematical techniques, such as the Padé method, the numerical methods and so forth. Especially, unlike other analytic techniques, the homotopy analysis method itself provides a convenient way to control and adjust the convergence of solutions series<sup>[33]</sup>. Some new solutions have been found by means of the homotopy analysis method<sup>[34]</sup>, which were never reported even by means of numerical techniques. Thanks to these advantages, it has been widely applied to many aspects of nonlinear problems<sup>[33-41]</sup>. In the next section, we present the solution process of the homotopy analysis method.

## 1 Homotopy analysis method

Let's define the (jointly continuous) maps  $F(\eta; q) \mapsto f(\eta)$  and  $\Theta(\eta; q) \mapsto \theta(\eta)$ , where the embedding parameter  $q \in [0, 1]$ , such that, as  $q$  increases from 0 to 1,  $F(\eta; q)$  and  $\Theta(\eta; q)$  vary from the initial guesses

to the exact solutions  $f(\eta)$  and  $\theta(\eta)$ , respectively. To ensure this, we construct the following *zero-order deformation equations* of the governing equations:

$$(1-q)L_f[F(\eta; q) - f_0(\eta)] = \hbar q N_f[F(\eta; q)], \quad (17)$$

$$(1-q)L_\theta[\Theta(\eta; q) - \theta_0(\eta)] = \hbar q N_\theta[F(\eta; q), \Theta(\eta; q)], \quad (18)$$

where  $\hbar \neq 0$  is a convergence-control parameter<sup>[41]</sup> which helps ensure the convergence of the solution series; the operator  $N_f[F(\eta; q)]$  is defined by the governing equation (4) or (7);  $N_\theta[F(\eta; q), \Theta(\eta; q)]$  is defined by the governing equation (10) or (11) depending on the two-dimensional or the three-dimensional case. A parameter  $\lambda = 1, 2$  is introduced so that either  $N_f$  or  $N_\theta$  can be expressed by

$$N_f[F(\eta; q)] := \frac{\partial^3 F}{\partial \eta^3} + \lambda F \frac{\partial^2 F}{\partial \eta^2} - \left( \frac{\partial F}{\partial \eta} \right)^2 + 1, \quad (19)$$

$$N_\theta[F(\eta; q), \Theta(\eta; q)] := \frac{\partial^2 \Theta}{\partial \eta^2} + \lambda \text{Pr} F \frac{\partial \Theta}{\partial \eta}. \quad (20)$$

Here,  $\lambda = 1$  corresponds to the two-dimensional flow and  $\lambda = 2$  corresponds to the axisymmetric flow. The boundary conditions (8), (13) and (14) yield

$$F(0; q) = 0, \quad \frac{\partial F}{\partial \eta}(\infty; q) - 1 = 0, \quad \Theta(\infty; q) = 0, \quad (21)$$

$$\frac{\partial F}{\partial \eta}(0; q) - \ell \frac{\partial^2 F}{\partial \eta^2}(0; q) = 0, \quad (22)$$

$$\Theta(0; q) - \beta \frac{\partial \Theta}{\partial \eta}(0; q) - 1 = 0. \quad (23)$$

$L_f$  and  $L_\theta$  are auxiliary linear operators defined by

$$L_f := \frac{\partial^3}{\partial \eta^3} - \frac{\partial}{\partial \eta}, \quad (24)$$

$$L_\theta := \frac{\partial^2}{\partial \eta^2} + \frac{\partial}{\partial \eta}. \quad (25)$$

Clearly, when  $q = 0$ , the zero-order deformation equations (17), (18) and (21) to (23) give rise to

$$F(\eta; 0) = f_0(\eta), \quad \Theta(\eta; 0) = \theta_0(\eta). \quad (26)$$

When  $q = 1$ , they become

$$F(\eta; 1) = f(\eta), \quad \Theta(\eta; 1) = \theta(\eta). \quad (27)$$

Here,  $f_0(\eta)$  and  $\theta_0$  are initial guesses. It is known that the boundary-layer flows velocity and temperature distributions are exponential decaying; therefore, it is

reasonable to assume that both  $f(\eta)$  and  $\theta(\eta)$  contain the exponential function. Secondly, according to the second equation in eq. (21),  $f_0(\eta)$  cannot be expressed by pure exponential functions only. It needs some kind of function which has the property that the first derivative is 1. Thus we can assume the initial guess of  $f(\eta)$  is

$$f_0(\eta) = c_1 + \eta + c_2 \exp(-\eta),$$

where  $c_1$  and  $c_2$  are constants to be determined by the first equation in eqs. (21) and (22), such that

$$f_0(\eta) = -\frac{1}{1+\ell} + \eta + \frac{1}{1+\ell} \exp(-\eta). \quad (28)$$

The initial guess of  $\theta(\eta)$  is simple. We can assume  $\theta_0(\eta) = d_1 \exp(-\eta)$ , with the constant  $d_1$  being determined by eq. (23), such that

$$\theta_0(\eta) = \frac{1}{1+\beta} \exp(-\eta). \quad (29)$$

The above pair of initial guesses are not the only one. But they are direct and simple. In sec. 2, we will show that the initial guesses have little impact on the final solution as long as the homotopy solutions proceed to high orders.

Expanding  $F(\eta; q)$  and  $\Theta(\eta; q)$  in Maclaurin series with respect to the embedding parameter  $q$ , we obtain

$$F(\eta; q) = f_0(\eta) + \sum_{n=1}^{\infty} f_n(\eta) q^n, \quad (30)$$

$$\Theta(\eta; q) = \theta_0(\eta) + \sum_{n=1}^{\infty} \theta_n(\eta) q^n, \quad (31)$$

where

$$f_n(\eta) = \frac{1}{n!} \frac{\partial^n}{\partial q^n} F(\eta; 0), \quad \theta_n(\eta) = \frac{1}{n!} \frac{\partial^n}{\partial q^n} \Theta(\eta; 0). \quad (32)$$

Assuming that above series converges at  $q = 1$ , we have

$$f(\eta) = f_0(\eta) + \sum_{n=1}^{\infty} f_n(\eta), \quad (33)$$

$$\theta(\eta) = \theta_0(\eta) + \sum_{n=1}^{\infty} \theta_n(\eta). \quad (34)$$

Differentiating the zero-order deformation equations (17), (18) and (21) to (23)  $m$  times with respect to  $q$ , then setting  $q=0$ , and finally dividing by  $m!$ , we have the high-order deformation equations ( $m \geq 1$ ):

$$L_f[f_m - \chi_m f_{m-1}] = \hbar R_m, \quad (35)$$

$$L_\theta[\theta_m - \chi_m \theta_{m-1}] = \hbar S_m, \quad (36)$$

with the boundary conditions:

$$f_m(0) = 0, \quad f'_m(\infty) = 0, \quad \theta_m(\infty) = 0, \quad (37)$$

$$f'_m(0) - \ell f''_m(0) = 0, \quad (38)$$

$$\theta_m(0) - \beta \theta'_m(0) = 0, \quad (39)$$

where

$$\chi_m = \begin{cases} 0, & m = 1; \\ 1, & m > 1, \end{cases} \quad (40)$$

and

$$R_m = f'''_{m-1} + \lambda \sum_{i=0}^{m-1} f_i f''_{m-1-i} - \sum_{i=0}^{m-1} f'_i f'_{m-1-i} + 1 - \chi_m, \quad (41)$$

$$S_m = \theta''_{m-1} + \lambda Pr \sum_{i=0}^{m-1} f_i \theta'_{m-1-i}. \quad (42)$$

Then the solutions for eqs. (35) and (36) can be expressed by

$$f_m(\eta) = \chi_m f_{m-1} + \hbar L_f^{-1}[R_m] + C_0 + C_1 \exp(\eta) + C_2 \exp(-\eta), \quad (43)$$

$$\theta_m(\eta) = \chi_m \theta_{m-1} + \hbar L_\theta^{-1}[S_m] + D_0 + D_1 \exp(-\eta), \quad (44)$$

where  $C_i, D_i$  are the five integral constants to be determined by the five boundary conditions (37) to (39),  $L_f^{-1}$  and  $L_\theta^{-1}$  denote the inverse linear operators of  $L_f$  and  $L_\theta$  so that the problem is closed. For example, solving the 1st-order deformation equation, we have

$$f_1(\eta) = \frac{\hbar}{12(1+\ell)^3} \times [A_{1,0} + A_{1,1} \exp(-\eta) + A_{1,2} \exp(-2\eta)], \quad (45)$$

$$\theta_1(\eta) = \frac{\hbar}{4(1+\ell)(1+\beta)^2} \times [B_{1,1} \exp(-\eta) + B_{1,2} \exp(-2\eta)] \quad (46)$$

where

$$A_{1,0} = -4 - 5\lambda - 12\ell^2(1+\lambda) - 3\ell(4+5\lambda),$$

$$A_{1,1} = 2 + 10\ell + 12\ell^2 + (7 + 17\ell + 12\ell^2)\lambda + 3(1+\ell)[2 + \lambda + \ell(2+3\lambda)]\eta + 3(1+\ell)^2 \lambda \eta^2,$$

$$A_{1,3} = 2(1+\ell)(1-\lambda), \quad (47)$$

and

$$B_{1,1} = -4(1+\ell)\eta + 2\lambda Pr[1 + \eta^2 + \ell\eta(2+\eta)] - 2\beta\{2(1+\ell)(1+\eta) - \lambda Pr[2 + \eta^2 + \ell(2+2\eta + \eta^2)]\}$$

$$B_{1,2} = -2 \lambda Pr (1 + \beta). \quad (48)$$

With the aid of mathematical software, such as *Mathematica*, it is easy to proceed to high orders.

## 2 Results and discussions

Note that the series solutions (33) and (34) contain the convergence-control parameter  $\hbar$ . But if we apply the homotopy Padé method<sup>[32,42]</sup>,  $\hbar$  disappears in our results. The homotopy Padé method can largely accelerate the convergence of solution series. Also, it plays the role of a filter which filters out the most slowly decaying factors so as to accelerate the transient process and makes it stable. To show its advantages, we compare the  $[m,m]$  homotopy Padé approximants and numerical results of  $\theta'(0)$  for the axisymmetric flow with the differential equations (11), (13) and (14) when  $Pr=0.7$  in Tables 1 and 2. It can be seen the  $[m,m]$  homotopy Padé approximants converge and agree well with the numerical results.

Comparisons among the  $[20,20]$  homotopy Padé approximants, the numerical integrations using shooting method and the asymptotic approximations for  $\theta'(0)$  in eqs. (15) and (16) are shown in Figures 1 and 2 for the two-dimensional and the three-dimensional flows where  $Pr=0.7$  and  $Pr=7$ . The Prandtl numbers of 0.7 and 7 represent air and water, respectively. For fixed  $\ell$  the thermal initial value  $\theta'(0)$  decreases in magnitude as the slip thermal slip factor  $\beta$  increases. For fixed  $\beta$  the thermal initial value increases in magnitude but the rate of change decreases as the slip length  $\ell$  increases. It is seen the  $[20,20]$  homotopy Padé approximants agree well with the numerical results. When  $\ell$  and  $\beta$  are small, the asymptotic approximations for  $\theta'(0)$  in eqs.

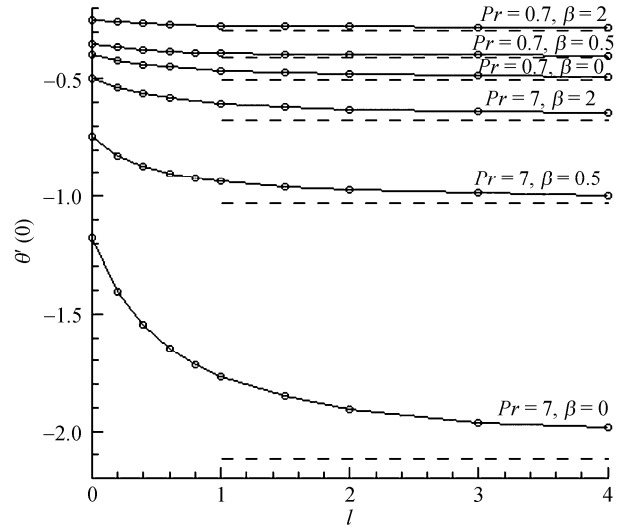


**Figure 1** Thermal initial values for the two-dimensional stagnation flow. The solid:  $[20,20]$  homotopy Padé approximant; the circle: numerical result; the dashed: asymptotic approximation (15).

(15) and (16) look too crude.

Recall that we have freedom to choose the initial guesses. We use the initial guesses (28) and (29) in our analysis so far. But what if we use some other pairs of initial guesses? Do they affect the convergence of the final solutions? To answer it, we compare the initial guess chosen in the same way as we explained in sec. 1, such that

$$\begin{aligned} f_0(\eta) &= -\frac{1}{(1+n\ell)n} + \eta + \frac{1}{(1+n\ell)n} \exp(-n\eta), \\ \theta_0(\eta) &= \frac{1}{1+k\beta} \exp(-k\eta), \quad n, k = 1, 2, 3, \dots \end{aligned} \quad (49)$$

**Table 1** The  $[m,m]$  homotopy Padé approximant of  $\theta'(1)$  for the axisymmetric flow for  $Pr=0.7, \beta=0$  and different  $\ell$

$[m,m]$	$\ell=0$	$\ell=0.2$	$\ell=0.4$	$\ell=1$	$\ell=2$	$\ell=3$
[15,15]	-0.6651	-0.7365	-0.7818	-0.8484	-0.8879	-0.9044
[16,16]	-0.6652	-0.7366	-0.7820	-0.8484	-0.8879	-0.9044
[17,17]	-0.6653	-0.7365	-0.7818	-0.8483	-0.8879	-0.9044
[18,18]	-0.6654	-0.7365	-0.7818	-0.8483	-0.8879	-0.9044
[19,19]	-0.6655	-0.7365	-0.7818	-0.8483	-0.8879	-0.9044
[20,20]	-0.6654	-0.7365	-0.7818	-0.8483	-0.8879	-0.9044
numerical	-0.6654	-0.7365	-0.7818	-0.8483	-0.8879	-0.9044

**Table 2** The  $[m,m]$  homotopy Padé approximant of  $\theta'(1)$  for the axisymmetric flow for  $Pr=0.7, \beta=2$  and different  $\ell$

$[m,m]$	$\ell=0$	$\ell=0.2$	$\ell=0.4$	$\ell=1$	$\ell=2$	$\ell=3$
[15,15]	-0.2854	-0.2978	-0.3050	-0.3146	-0.3199	-0.3220
[16,16]	-0.2854	-0.2978	-0.3050	-0.3146	-0.3199	-0.3220

[17,17]	-0.2855	-0.2978	-0.3050	-0.3146	-0.3199	-0.3220
[18,18]	-0.2855	-0.2978	-0.3050	-0.3146	-0.3199	-0.3220
[19,19]	-0.2855	-0.2978	-0.3050	-0.3146	-0.3199	-0.3220
[20,20]	-0.2855	-0.2978	-0.3050	-0.3146	-0.3199	-0.3220
numerical	-0.2855	-0.2978	-0.3050	-0.3146	-0.3199	-0.3220

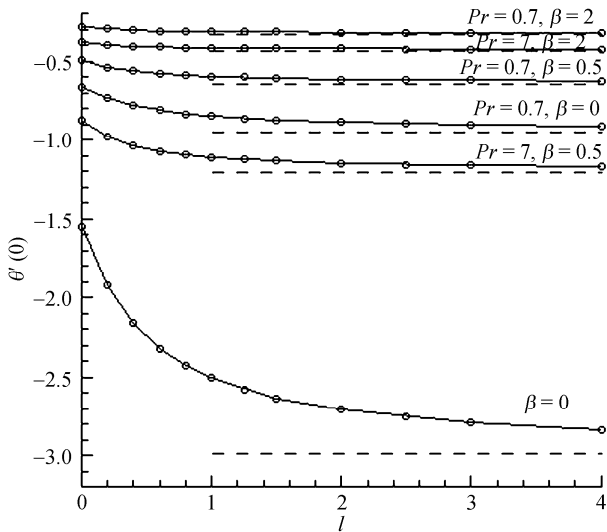


**Figure 2** Thermal initial values for the axisymmetric stagnation flow. The solid: [20,20] homotopy Padé approximant; the circle: numerical result; the dashed: asymptotic approximation (16).

Table 3 shows a comparison between the initial guesses when  $n=k=4$  and when  $n=k=1$  (eqs. (28) and (29)) for the discussed three-dimensional flows. It is seen that the initial guesses have little impact on the final solutions as long as they proceed to high orders.

**Table 3** A comparison of the  $[m,m]$  homotopy Padé approximant of  $\theta'(1)$  with different initial guesses in eq. (49) where  $n=k=1$  and  $n=k=4$ , respectively, for the axisymmetric flow when  $Pr=0.7$ ,  $\beta=2$  and  $\ell=1$

$[m,m]$	$n=k=1$	$n=k=4$
[2,2]	-0.3389	-0.3307
[4,4]	-0.3083	-0.3182
[6,6]	-0.3135	-0.3156
[8,8]	-0.3141	-0.3149
[10,10]	-0.3145	-0.3146
[20,20]	-0.3146	-0.3146

### 3 Conclusion

A relatively new analytic method, namely, the homotopy analysis method is applied to examine the problem of

nano thermal boundary layers with slip boundary conditions. Convergent high-order solutions are obtained for similar equations of the two-dimensional and three-dimensional axisymmetric stagnation flow. The present method is based on a continuous variation from an initial trial to the exact solution. It does not rely on the expansion of any small/large physical parameters so that it is theoretically applicable for not only weak but also strong nonlinear flow phenomena. To accelerate the convergence rate, the homotopy Padé technique is also applied. The  $[m,m]$  homotopy Padé approximants are compared with the numerical results using shooting method and the asymptotic approximations. It is found that the homotopy Padé approximants are independent of the convergence-control parameter  $\hbar$ ; therefore, the solution approximations are always convergent by means of this approach, though it is a pity that we have no strict general proof. The homotopy Padé approximants agree well with the numerical results.

Effects of the flow slip length  $\ell$ , the thermal slip constant  $\beta$ , and the Prandtl numbers  $Pr$  on the heat transfer characteristics are investigated. It is found that the thermal initial  $\theta'(0)$  increases in magnitude with the increased flow slip length  $\ell$ , increased Prandtl number and decreased thermal slip constant  $\beta$ . When  $\ell$  approaches to infinity,  $\theta'(0)$  has an asymptotic property: eq. (15) for two-dimensional flow and eq. (16) for axisymmetric flow.

From Figures 1 and 2 and Tables 1 and 2, the rate of the heat transfer is more pronounced when there is a velocity slip between the solid wall and the flow adjacent to it. This behavior is more true in the high viscous fluid (water) case than in the low viscous fluid (air) case. Quite opposite is the case, when there is a thermal jump at solid interfaces. Moreover, negative values of  $\theta'(0)$  physically indicate that the heat flow is always from the wall to the fluid.

- 1 Fisher E G. Extrusion of Plastics. New York: Wiley, 1976
- 2 Schlichting H. Boundary Layer Theory. New York: McGraw-Hill, 1979
- 3 Tropea C, Yarin A L, Foss J F. Microfluidics: The no-slip boundary condition. In: Handbook of Experimental Fluid Mechanics, Chapter 19.

- Berlin Heidelberg: Springer, 2007
- 4 Neto C, Evans E, Bonaccorso E, et al. Boundary slip in newtonian liquids: A review of experimental studies. Rep Prog Phys, 2005, 68: 2859–2897
- 5 Jennissen H P. Boundary-layer exchange by bubble: A novel method

- for generating transient nanofluidic layers. *Phys Fluids*, 2005, 17: 100616
- 6 White F M. *Viscous Fluid Flow*. 3rd ed. Boston: McGraw-Hill, 2006
  - 7 Navier C L M H. Mémoire sur les lois du mouvement des fluides. *Mémoires de l'Académie Royale des Sciences de l'Institut de France*, 1823, 6: 389–440
  - 8 Schaaf S, Chambre P. *Flow of Rarefied Gass*. Princeton: Princeton University Press, 1961
  - 9 Kaneta N, Nishikawa H, Kameishi K. Observation of wall slip in elasto-hydrodynamic lubrication. *ASME: J Tribol*, 1990, 112: 447–584
  - 10 Russel W B, Saville D A, Schowalter W R. *Colloidal Dispersions*. Cambridge: Cambridge University Press, 1989
  - 11 Batchelor G K. *An Introduction to Fluid Dynamics*. Cambridge: Cambridge University Press, 1967
  - 12 Von Smolushowski M. Ueber Wärmeleitung in verdünnten Gasen. *Ann Phys Chem*, 1898, 64: 101–130
  - 13 Wang C Y. Stagnation slip flow and heat transfer on a moving plate. *Chem Eng Sci*, 2006, 61: 7668–7672
  - 14 Mathews M T, Hill J M. Micro/nano thermal boundary layer equations with slip-creep-jump boundary conditions. *IMA J Appl Math*, 2007, 72: 894–911
  - 15 Ishimura N, Ushijima T K. An elementary approach to the analysis of exact solutions for the Navier-Stokes stagnation flows with slips. *Arch Math*, 2004, 82: 432–441
  - 16 Nayfeh A H. *Perturbation Methods*. New York: John Wiley & Sons, 1973
  - 17 Van Dyke M D. *Perturbation Methods in Fluid Mechanics*. New York: Academic, 1964
  - 18 Von Dyke M D. *Perturbation Methods in Fluid Mechanics*. Stanford: The Parabolic Press, 1975
  - 19 Nayfeh A H. *Introduction to Perturbation Techniques*. New York: John Wiley & Sons, 1981
  - 20 Nayfeh A H. *Problems in Perturbation*. New York: John Wiley & Sons, 1985
  - 21 Murdock J A. *Perturbations: Theory and Methods*. New York: John Wiley & Sons, 1991
  - 22 Nayfeh A H. *Method of Normal Forms*. New York: John Wiley & Sons, 1993
  - 23 Nayfeh A H. *Perturbation Methods*. New York: John Wiley & Sons, 2000
  - 24 Poincaré H. *Les méthodes nouvelles de la mécanique*. Paris: Gauthier-Villars, 1892
  - 25 Lyapunov A M. *General problem on stability of motion (English translation)*. London: Taylor & Francis, 1992
  - 26 Karmishin A V, Zhukov A T, Kolosov V G. *Methods of dynamics calculation and testing for thin-walled structures (in Russian)*. Moscow: Mashinostroyeniye, 1990
  - 27 Awrejcewicz J, Andrianov I V, Manevitch L I. *Asymptotic Approaches in Nonlinear Dynamics*. Berlin: Springer-Verlag, 1998
  - 28 Adomian G. *Nonlinear Stochastic Differential Equations*. *J Math Anal Applic*, 1976, 55: 441–452
  - 29 Adomian G, Rach R. On the solution of algebraic equations by the decomposition method. *Math Anal Appl*, 1985, 105(1): 141–166
  - 30 Cherruault Y. Convergence of Adomian's method. *Kybernetika*, 1988, 8(2): 31–38
  - 31 Adomian G. A review of the decomposition method and some recent results for nonlinear equations. *Comp Math Applic*, 1991, 21: 101–127
  - 32 Liao S J. *Beyond Perturbation: Introduction to the Homotopy Analysis Method*. Boca Raton: Chapman & Hall/CRC Press, 2003
  - 33 Liang S, Jeffrey D J. Comparison of homotopy analysis method and homotopy perturbation method through an evaluation equation. *Commun Nonlinear Sci Numer Simul*, online, doi: 10.1016/j.cnsns.2009.02.016
  - 34 Liao S J, Magyari E. Exponentially decaying boundary layers as limiting cases of families of algebraically decaying ones. *Zeitschrift für angewandte Mathematik und Physik*, 2006, 57(5): 777–792
  - 35 Liao S J. *Beyond perturbation: the homotopy analysis method and its application*. *Adv Mech*, 2008, 38(1): 1–34
  - 36 Liao S J, Tan Y. A general approach to obtain series solutions of nonlinear differential equations. *Stud Appl Math*, 2007, 119: 297–355
  - 37 Sajid M, Hayat T, Asghar S. Comparison between the HAM and HPM solutions of thin film flows of non-Newtonian fluids on a moving belt. *Nonlinear Dyn*, 2007, 50: 27–35
  - 38 Hayat T, Sajid M. On analytic solution for thin film flow of a fourth grade fluid down a vertical cylinder. *Phys Lett A*, 2007, 361: 316–322
  - 39 Marinca V, Herisanu N, Nemes I. A modified homotopy analysis method with application to thin film flow of a fourth grade fluid down a vertical cylinder. *Central Eur J Phys*, 2009, 14(4): 1196–1207
  - 40 Cheng J, Cang J, Liao S J. On the interaction of deep water waves and exponential shear currents. *Zeitschrift für angewandte Mathematik und Physik*, online, doi: 10.1007/s00033-008-7050-1
  - 41 Liao S J. Notes on the homotopy analysis method some definitions and theorems. *Commun Nonlinear Sci Numer Simul*, 2009, 14(4): 983–997
  - 42 Van Dyke M. Extension of Goldstein's series for the Oseen drag of a sphere. *J Fluid Mech*, 1970, 44: 365–372